Numerical Simulations and Experimental Verification of Laser Welding of Nylon 6

Santosh Kumar Gupta[1], Sanjib Jaypuria[1], Dilip Kumar Pratihar[2], Partha Saha[2]

1. The Advanced Technology Centre, IIT Kharagpur, Kharagpur, West –Bengal/India
2. Mechanical Engineering Department, IIT Kharagpur, Kharagpur, West –Bengal/India

Abstract

Laser welding is often considered to be a superior technique compared to conventional welding methods and it has been gradually evolved into an efficient manufacturing process. It is a high energy density fabrication process and generally employed for fabricating intricate shapes/contours in polymers with the better precision. Nylon 6 is a semi-crystalline polymer and is manufactured artificially to impart desirable properties. Due to its high durability, strength, and temperature resistant properties, Nylon 6 is often used as an engineering thermoplastic. In the past, joining of metals and polymers was carried out by keeping the laser beam fixed at a point and temperature distribution along the different axes was the main concerned area of analysis whereas a limited attention was given to weld bead prediction and residual stress analysis. Therefore, in this work, a three-dimensional (3D) time-dependent model was implemented using a finite element approach and the process of welding is simulated in COMSOL Multiphysics. Unreinforced Nylon 6 specimens were fabricated using a moving laser beam (Gaussian heat source) for a lap-joint geometry. The results of the numerical analysis were validated through experimental data. For making the thermo-mechanical analysis more realistic, it was carried out by varying the physical properties, viz., density, thermal conductivity, specific heat, Young's modulus, coefficient of thermal expansion and Poisson's ratio over a range of temperature to ensure accuracy in numerical analysis. Heat transfer in solid and thermal stress were the two modules that were used for the analysis of weld-bead geometry and residual stress. The weld seam dimensions, viz., penetration depth (PD) and weld width (WW) were found to increase with an increase in the beam radius. The amount of residual stress is mainly affected by scanning velocity.

Keywords: Transmission laser welding; Line energy; Mushy phase; Nylon 6; Weld bead geometry.

1. Introduction

Plastics are flourishing material due to its characteristics like portability, corrosion resistance and weather resistance. Nylon 6 is highly resistant to temperature, abrasion and chemicals. It possesses properties, such as toughness, high tensile strength and elasticity as compared to other polymers, which has lead to extensive use of this polymer in automobiles, manufacturing industries and industrial yarn. Laser welding produces quality welds but due to huge investments required initially, the process was not economically viable. Laser welding of polymers demonstrated its application in manufacturing by proving itself as an alternative to previously used fabrication methods. Therefore, it went through regressive research in the last few decades. Lap joint is the most preferable configuration for the welding of polymers. The quality of joint obtained in the welding of plastics depends upon the amount of heat input given to the interface to create melt-pool. In through transmission laser welding, the two sheets to be welded are joined by heat conduction from opaque sheet to the transparent sheet. The heat input is localized that results into residual stresses after cooling takes place. The present work compares the experimental results of through-transmission laser welding of Nylon 6 sheets by lap joint with that of numerical analysis.

2. Governing Equations

The heat equation (1) for the simulation includes convective terms to quantify temperature over the whole geometry, as given below

$$\rho C_P \frac{\partial T}{\partial t} + \rho C_P \mathrm{u}\nabla \mathrm{T} = \nabla\left(k\nabla T\right) + q_v, \quad (1)$$

where ρ is the density, C_p is the specific heat, u is the velocity field, k is the thermal conductivity, T is the temperature and q_v is the volumetric heat generated by laser. The mushy phase is taken into by considering the equivalent specific heat method. The other two modes of heat transfer taken into account are convection and radiation. The heat losses from the surfaces are given by the equation (2).

$$q = h(Ts - To) + \sigma\varepsilon(Ts^4 - To^4), \quad (2)$$

where q is total heat loss by convection and radiation, T_s is the surface temperature and T_o is the ambient temperature. Convective heat transfer coefficient is denoted by h. Material emissivity and Stefan Boltzmann constant are denoted by ε and σ, respectively. The analysis of variation of residual stress along the transverse direction of the scanning direction of laser is done to know the type of stress, i.e., tensile or compressive induced after the welding of two polyamide sheets. The thermal stresses induced are governed by the equations (3), (4), (5) and (6).

$$\varepsilon = \frac{1}{2}[(\nabla u)^T + \nabla u], \quad (3)$$

where ε is the symmetric strain tensor. The equilibrium equations of solid mechanics follow the Newton's second law, which, if neglecting inertial terms, can be written as

$$0 = \nabla\sigma + Fv \quad (4)$$

Stress tensor and body force vector are denoted by σ and Fv, respectively . Stress tensor is related to the elastic strain tensor $\in_{EL}$ by the Hooke's law:

$$\in_{EL} = \varepsilon - \varepsilon_{th} \quad (5)$$

$$\sigma = C(E,v): \in_{EL}$$

$$= C(E,v): (\varepsilon - \varepsilon_{th}) \quad (6)$$

Elasticity tensor $C(E,v)$ for an isotropic material is given by the mechanical properties (material constants), such as elastic modulus and Poisson's ratio. The thermal strain induced ε_{th}can be calculated by equation (7).

$$\varepsilon_{th} = \propto \left(T - T_{ref}\right), \quad (7)$$

where $\propto$ is the coefficient of thermal expansion. T_{ref} is the ambient temperature and T is the working temperature.

3. Experiment and Simulation of Laser Welding

The present work deals with TTLW of Nylon 6. The three welding parameters that were used to weld Nylon 6 sheet in lap joints configuration [1] using diode laser and then, simulated by COMSOL Multiphysics are tabulated in Table 1. Each welded joint constitutes of one transparent sheet and one opaque sheet each [2]. Dimensions of each sample are 50 mm x 50 mm x 3 mm, as shown in Fig 1. Diode laser (Neodymium-doped yttrium orthovanadate (Nd:YVO_4) with maximum output power of 9.28 W was used for conducting welding experiments. The beam diameter used for welding experiment was kept constant at 0.05 mm, which was moved at the mid-point of the overlapped region, as indicated in Fig. 1. Laser power (P), scanning velocity (V) and frequency (F) [3, 4] were assorted in the intervals of 7 W to 9 W, 0.15 mm/s to 0.25 mm/s, and 4 KHz to 6 KHz, respectively. Fig. 1 shows the origins for three co-ordinate axes, i.e., X = 0 is located at the left end of the opaque part, laser beam scanning starts from Y = 0 and Z = 0 lies at the interface of the two sheets to be welded. From the interface of two sheets, the upward direction was considered to be positive coordinate (+) and downward direction to be negative coordinate (-).

For the numerical simulation, symmetric conditions that help in minimizing the simulation time, were considered. In the numerical analysis, overlapped portion consisted of the transparent (top) part and the opaque (bottom) part [6,8]. Conduction, convection and radiation were considered as the mode of heat transfer for numerical computation. Multilinear isentropic hardening model was applied to study residual stress-strain behaviour. Temperature (T) dependent physical properties, viz., density (ρ), thermal conductivity (k), specific heat (C_p), Young's modulus (E), coefficient of thermal expansion (α) and Poisson's ratio (μ) were used in thermal modeling.

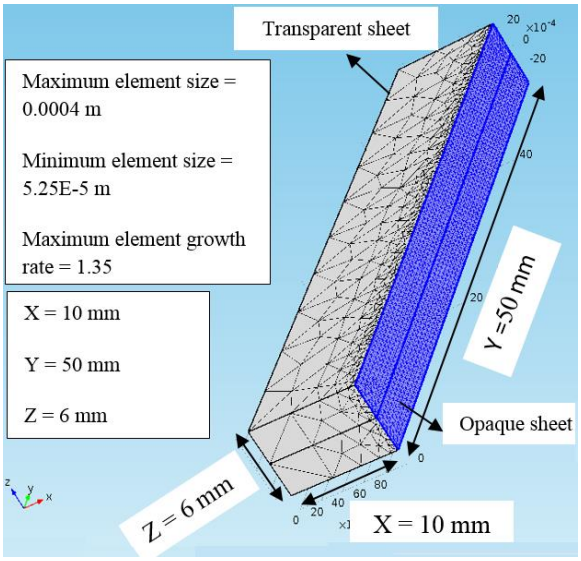

Figure 1. Discretized region of the overlapped portion

4. Results and Discussion

The bead profile formed at the fusion zone was analyzed to measure the penetration depth and weld width. Penetration depth was measured by plotting the variation of temperature along thickness of the two overlapped sheets as shown in Fig. 3. The

comparison between the simulated data and experimental results are tabulated in Table 1. The proportion of penetration depth to weld width is defined as aspect ratio. Line energy is the ratio of laser power to scanning velocity. When the input parameters considered for the experiment were 7 W, 0.20 mm/s and 5 KHz, it resulted into line energy of 35 J/mm and aspect ratio of 1.75. However, when the parameters were varied to 9 W, 0.15 mm/s and 4 KHz, there was an increment in line energy and aspect ratio. Line energy of the second condition was 60 J/mm and aspect ratio improved by 0.11. It was observed that there was an increase in the aspect ratio with an increase of the line energy. The phases that are found to occur in Nylon 6 are α and ϒ phases [9,10]. Nylon 6 are mainly composed of these two phases. The α phase shows the anti-parallel chains, whereas in ϒ phase, the parallel chains are evitable. The peak for ϒ phase is found to occur at 2θ = 21.72 and α phase is present at 2θ = 24.1047 [5], which is depicted in Fig. 2. Residual thermal stresses get induced due to solidification after melting in the welded zone. The thermal stresses along the transverse direction of the scanning direction of the laser source were measured and compared to the stresses quantified by numerical analysis. The thermal stress measured across the transverse direction of welding path reflects that the stress induced in fusion zone increases in the range of 9.268-11.029 MPa, as the line energy escalates from 35 J/mm to 60 J/mm. It can be concluded that induced thermal stresses showed an increasing trend with an increase of line energy. Fig. 4 demonstrates the stress variation along the interface of the two sheets in the transverse direction, i.e., X axis. It is observed that there is overall 15 % of error between the simulated and experimental results of penetration depth (PD), weld width (WW) and residual stress [7].

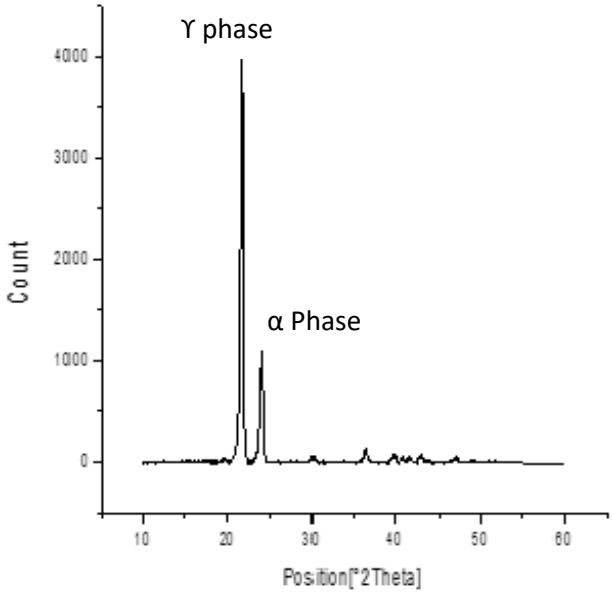

Figure 2. XRD phase analysis of Nylon 6

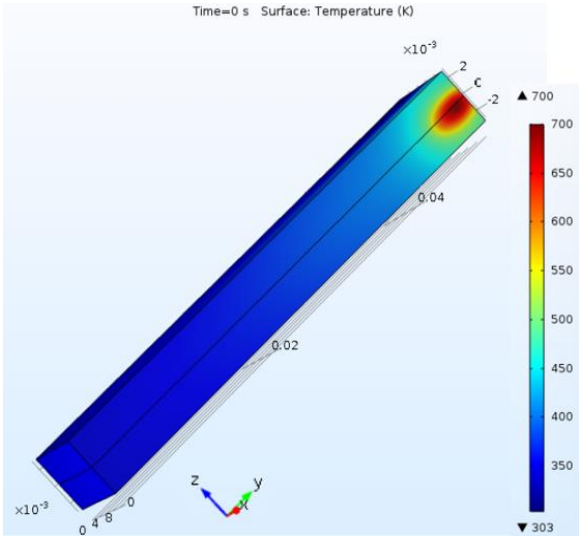

Figure 3. Temperature distribution at the interface of the two sheets

Table 1 - Comparison between experimental and simulated results for different combination of input parameters

Sl. no	P (W)	V (mm/s)	F (kHz)	Expt. PD (mm)	Simulated PD (mm)
1	7	0.20	5	2.954	3.451
2	8	0.15	5	3.287	3.860
3	9	0.15	4	3.615	4.252
Sl. no	P (W)	V (mm/s)	F (kHz)	Expt. WW (mm)	Simulated WW (mm)
1	7	0.20	5	1.682	1.961
2	8	0.15	5	1.774	2.059
3	9	0.15	4	1.941	2.283
Sl. no	P (W)	V (mm/s)	F (kHz)	Expt. Stress (MPa)	Simulated Stress (MPa)
1	7	0.20	5	9.268	10.66
2	8	0.15	5	10.481	11.54
3	9	0.15	4	11.029	11.88

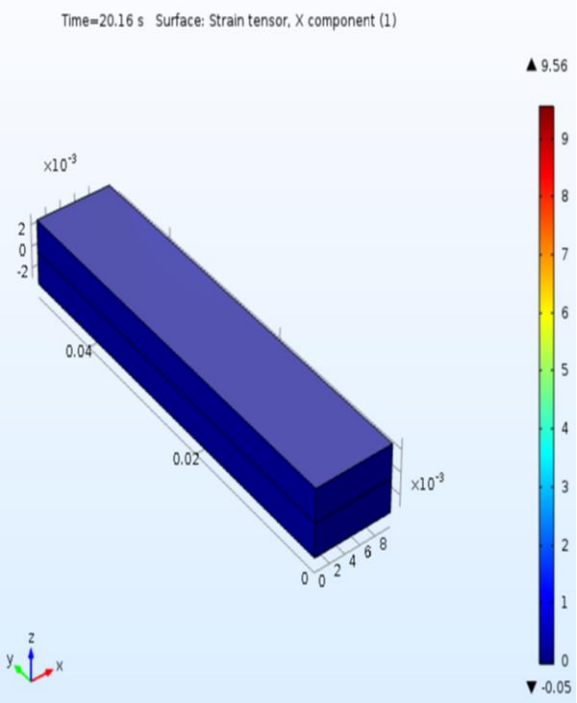

Figure 4. Stress variation at the interface of the two sheets

5. Conclusions

Nylon 6 sheets were welded in pulse mode of laser welding. Experimental work and numerical analysis were carried out by providing the identical input parameters and boundary conditions in both the earlier mentioned methods. Heat transfer in solid and thermal stress were used to model the whole process by numerical analysis to quantify the dimensions of weld-bead and thermal stresses induced after welding. The results of experimental work and numerical analysis when compared, it is found that there is a difference of 15% between them. This shows that there is a good agreement between the experimental data and simulated results. Considering the accuracy in the simulation, the perspective work can be used to model conduction and keyhole modes of laser welding for different metals and non-metals, such as polymers in automobile industry, structural materials used in fabrication in power plants and chemical industries, which is quite expensive. Numerical analysis helps in reducing the number of experiments and thus, helps in reducing the wastage of resources.

6. References

[1] Pagano N., Campana G., Fiorina M., Morelli R. Laser transmission welding of polylactide to aluminium thin films for applications in the food-packaging industry. Optics & Laser Technology 2017; 91:80-84.

[2] Acherjee B, Kuar A. S., Mitra S, Misra D. Modeling of laser transmission contour welding process using FEA and DoE. Optics & Laser Technology 2012; 44: 1281-1289.

[3] Prabhakaran R., Kontopoulou M, Zak G, Bates P.J, Baylis B. K. Contour Laser- Laser-transmission Welding of Glass reinforced Nylon posite Materials. Journal of Thermoplast 2006; 19: 427-439.

[4] Wang X., Chen H., Liu H., Li P., Yan Z., Huang C., Zhao Z., Gu Y. Simulation and optimization of continuous laser transmission welding between PET and titanium through FEM, RSM, GA and experiments. Optics & Laser Technology 2013; 51: 1245-1254.

[5] Millot C. Multi-scale characterization of deformation mechanisms of bulk polyamide 6 under tensile stretching below and above the glass transition. Doctor of Philosophy's Thesis. National Institute of Applied Sciences of Lyon. https://tel.archives-ouvertes.fr/tel-01207840/ 2015 (accessed 29th May 2018).

[6] Azhikannickal E., Bates P.J., Zak G. Laser Light Transmission Through Thermoplastic as a function of Thickness and Laser Incidence Angle: Experimental and Modeling. Journal of Manufacturing Science and Engineering 2012; 134: 1-6.

[7] Tomashchuk I., Bendaoud I., Sallamand P., Cicala E., Lafaye S., Almuneau M. Multiphysical modelling of keyhole formation during dissimilar laser welding. Proceedings of the COMSOL Conference 2016; 1-7.

[8] Mayboudi L.S., Birk A.M., Zak G., Bates P.J. Laser Transmission Welding of a Lap-Joint: Thermal Imaging Observations and Three–Dimensional Finite Element Modeling. Journal of Heat Transfer 2007; 129: 1177-1186.

[9] Murthy N.S., Bray R.G., Correale S.T., Moore A.F. Drawing and annealing of nylon-6 fibres: studies of crystal growth, orientation of amorphous and crystalline domains and their

influence on properties. POLYMER 1995; 36: 3863-3873.

[10] Murthy N.S. Analysis of Meridional X-Ray Diffraction Pattern of the γ Form of Nylon 6 and Comparison of Paracrystalline and Microstrain Models of Lattice Disorder. Journal of Polymer Science: Part B: Polymer Physics 1986; 24: 549-561.